

University of Mississippi

eGrove

Faculty and Student Publications

Physics and Astronomy

3-23-2021

Evidence for $X(3872) \rightarrow j/\psi \pi^+ \pi^-$ Produced in Single-Tag Two-Photon Interactions

Y. Teramoto

Osaka Metropolitan University

S. Uehara

The Graduate University for Advanced Studies

M. Masuda

Osaka University

I. Adachi

The Graduate University for Advanced Studies

H. Aihara

The University of Tokyo

See next page for additional authors

Follow this and additional works at: https://egrove.olemiss.edu/physics_facpubs



Part of the [Astrophysics and Astronomy Commons](#)

Recommended Citation

Teramoto, Y., Uehara, S., Masuda, M., Adachi, I., Aihara, H., Al Said, S., Asner, D. M., Atmacan, H., Aushev, T., Ayad, R., Babu, V., Behera, P., Beleño, C., Bennett, J., Bhardwaj, V., Bhuyan, B., Bilka, T., Biswal, J., Bonvicini, G., ... Belle Collaboration. (2021). Evidence for $x(3872) \rightarrow j/\psi \pi^+ \pi^-$ produced in single-tag two-photon interactions. *Physical Review Letters*, 126(12), 122001. <https://doi.org/10.1103/PhysRevLett.126.122001>

This Article is brought to you for free and open access by the Physics and Astronomy at eGrove. It has been accepted for inclusion in Faculty and Student Publications by an authorized administrator of eGrove. For more information, please contact egrove@olemiss.edu.

Authors

Y. Teramoto, S. Uehara, M. Masuda, I. Adachi, H. Aihara, S. Al Said, D. M. Asner, H. Atmacan, T. Aushev, R. Ayad, V. Babu, P. Behera, C. Belen, J. Bennett, V. Bhardwaj, B. Bhuyan, T. Bilka, J. Biswal, and G. Bonvicini

Evidence for $X(3872) \rightarrow J/\psi\pi^+\pi^-$ Produced in Single-Tag Two-Photon Interactions

Y. Teramoto⁶⁵, S. Uehara,^{19,15} M. Masuda,^{85,71} I. Adachi,^{19,15} H. Aihara,⁸⁶ S. Al Said,^{79,38} D. M. Asner,³ H. Atmacan,⁷ T. Aushev,²¹ R. Ayad,⁷⁹ V. Babu,⁸ P. Behera,²⁷ C. Beleño,¹⁴ J. Bennett,⁵¹ V. Bhardwaj,²⁴ B. Bhuyan,²⁵ T. Bilka,⁵ J. Biswal,³⁴ G. Bonvicini,⁹¹ A. Bozek,⁶¹ M. Bračko,^{48,34} T. E. Browder,¹⁸ M. Campajola,^{32,56} D. Červenkov,⁵ M.-C. Chang,¹⁰ P. Chang,⁶⁰ V. Chekelian,⁴⁹ A. Chen,⁵⁸ B. G. Cheon,¹⁷ K. Chilikin,⁴³ K. Cho,⁴⁰ S.-J. Cho,⁹³ S.-K. Choi,¹⁶ Y. Choi,⁷⁷ S. Choudhury,²⁶ D. Cinabro,⁹¹ S. Cunliffe,⁸ G. De Nardo,^{32,56} F. Di Capua,^{32,56} Z. Doležal,⁵ T. V. Dong,¹¹ S. Eidelman,^{4,64,43} T. Ferber,⁸ B. G. Fulsom,⁶⁶ R. Garg,⁶⁷ V. Gaur,⁹⁰ N. Gabyshev,^{4,64} A. Garmash,^{4,64} A. Giri,²⁶ P. Goldenzweig,³⁵ D. Greenwald,⁸¹ C. Hadjivasiliou,⁶⁶ T. Hara,^{19,15} O. Hartbrich,¹⁸ K. Hayasaka,⁶³ H. Hayashii,⁵⁷ M. T. Hedges,¹⁸ M. Hernandez Villanueva,⁵¹ W.-S. Hou,⁶⁰ C.-L. Hsu,⁷⁸ T. Iijima,^{55,54} K. Inami,⁵⁴ G. Inguglia,³⁰ A. Ishikawa,^{19,15} R. Itoh,^{19,15} M. Iwasaki,⁶⁵ Y. Iwasaki,¹⁹ W. W. Jacobs,²⁸ E.-J. Jang,¹⁶ S. Jia,¹¹ Y. Jin,⁸⁶ C. W. Joo,³⁶ K. K. Joo,⁶ J. Kahn,³⁵ A. B. Kaliyar,⁸⁰ K. H. Kang,⁴² G. Karyan,⁸ Y. Kato,⁵⁴ T. Kawasaki,³⁹ H. Kichimi,¹⁹ C. Kiesling,⁴⁹ B. H. Kim,⁷³ D. Y. Kim,⁷⁶ S. H. Kim,⁷³ Y.-K. Kim,⁹³ T. D. Kimmel,⁹⁰ K. Kinoshita,⁷ P. Kodyš,⁵ S. Korpar,^{48,34} D. Kotchetkov,¹⁸ P. Križan,^{44,34} R. Kroeger,⁵¹ P. Krokovny,^{4,64} T. Kuhr,⁴⁵ R. Kulasiri,³⁷ R. Kumar,⁷⁰ K. Kumara,⁹¹ A. Kuzmin,^{4,64} Y.-J. Kwon,⁹³ K. Lalwani,⁴⁷ J. S. Lange,¹² I. S. Lee,¹⁷ S. C. Lee,⁴² P. Lewis,² L. K. Li,⁷ Y. B. Li,⁶⁸ L. Li Gioi,⁴⁹ J. Libby,²⁷ K. Lieret,⁴⁵ Z. Liptak,⁹⁴ D. Liventsev,^{91,19} T. Luo,¹¹ C. MacQueen,⁵⁰ T. Matsuda,⁵² D. Matvienko,^{4,64,43} M. Merola,^{32,56} K. Miyabayashi,⁵⁷ H. Miyata,⁶³ G. B. Mohanty,⁸⁰ S. Mohanty,^{80,89} T. J. Moon,⁷³ T. Mori,⁵⁴ M. Mrvar,³⁰ R. Mussa,³³ E. Nakano,⁶⁵ M. Nakao,^{19,15} H. Nakazawa,⁶⁰ Z. Natkaniec,⁶¹ A. Natchii,¹⁸ M. Nayak,⁸² N. K. Nisar,³ S. Nishida,^{19,15} K. Ogawa,⁶³ S. Ogawa,⁸³ H. Ono,^{62,63} Y. Onuki,⁸⁶ P. Pakhlov,^{43,53} G. Pakhlova,^{21,43} S. Pardi,³² H. Park,⁴² S.-H. Park,⁹³ S. Patra,²⁴ S. Paul,^{81,49} T. K. Pedlar,⁴⁶ R. Pestotnik,³⁴ L. E. Piilonen,⁹⁰ T. Podobnik,^{44,34} V. Popov,²¹ E. Prencipe,²² M. T. Prim,³⁵ M. Ritter,⁴⁵ A. Rostomyan,⁸ N. Rout,²⁷ G. Russo,⁵⁶ D. Sahoo,⁸⁰ Y. Sakai,^{19,15} S. Sandilya,⁷ A. Sangal,⁷ L. Santelj,^{44,34} T. Sanuki,⁸⁴ V. Savinov,⁶⁹ G. Schnell,^{1,23} J. Schueler,¹⁸ C. Schwanda,³⁰ Y. Seino,⁶³ K. Senyo,⁹² M. E. Sevir,⁵⁰ M. Shapkin,³¹ V. Shebalin,¹⁸ J.-G. Shiu,⁶⁰ J. B. Singh,⁶⁷ E. Solovieva,⁴³ M. Starič,³⁴ Z. S. Stottler,⁹⁰ M. Sumihama,¹³ K. Sumisawa,^{19,15} T. Sumiyoshi,⁸⁸ W. Sutcliffe,² M. Takizawa,^{74,20} U. Tamponi,³³ F. Tenchini,⁸ M. Uchida,⁸⁷ T. Uglov,^{43,21} Y. Unno,¹⁷ S. Uno,^{19,15} P. Urquijo,⁵⁰ Y. Usov,^{4,64} R. Van Tonder,² G. Varner,¹⁸ A. Vinokurova,^{4,64} V. Vorobyev,^{4,64,43} E. Waheed,¹⁹ C. H. Wang,⁵⁹ E. Wang,⁶⁹ M.-Z. Wang,⁶⁰ P. Wang,²⁹ X. L. Wang,¹¹ M. Watanabe,⁶³ E. Won,⁴¹ X. Xu,⁷⁵ B. D. Yabsley,⁷⁸ S. B. Yang,⁴¹ H. Ye,⁸ J. Yelton,⁹ J. H. Yin,⁴¹ Z. P. Zhang,⁷² V. Zhilich,^{4,64} V. Zhukova,⁴³ and V. Zhulanov^{4,64}

(Belle Collaboration)

¹University of the Basque Country UPV/EHU, 48080 Bilbao²University of Bonn, 53115 Bonn³Brookhaven National Laboratory, Upton, New York 11973⁴Budker Institute of Nuclear Physics SB RAS, Novosibirsk 630090⁵Faculty of Mathematics and Physics, Charles University, 121 16 Prague⁶Chonnam National University, Gwangju 61186⁷University of Cincinnati, Cincinnati, Ohio 45221⁸Deutsches Elektronen-Synchrotron, 22607 Hamburg⁹University of Florida, Gainesville, Florida 32611¹⁰Department of Physics, Fu Jen Catholic University, Taipei 24205¹¹Key Laboratory of Nuclear Physics and Ion-beam Application (MOE) and Institute of Modern Physics, Fudan University, Shanghai 200443¹²Justus-Liebig-Universität Gießen, 35392 Gießen¹³Gifu University, Gifu 501-1193¹⁴II. Physikalisches Institut, Georg-August-Universität Göttingen, 37073 Göttingen¹⁵SOKENDAI (The Graduate University for Advanced Studies), Hayama 240-0193¹⁶Gyeongsang National University, Jinju 52828¹⁷Department of Physics and Institute of Natural Sciences, Hanyang University, Seoul 04763¹⁸University of Hawaii, Honolulu, Hawaii 96822¹⁹High Energy Accelerator Research Organization (KEK), Tsukuba 305-0801²⁰J-PARC Branch, KEK Theory Center, High Energy Accelerator Research Organization (KEK), Tsukuba 305-0801²¹Higher School of Economics (HSE), Moscow 101000²²Forschungszentrum Jülich, 52425 Jülich

- ²³*IKERBASQUE, Basque Foundation for Science, 48013 Bilbao*
- ²⁴*Indian Institute of Science Education and Research Mohali, SAS Nagar, 140306*
- ²⁵*Indian Institute of Technology Guwahati, Assam 781039*
- ²⁶*Indian Institute of Technology Hyderabad, Telangana 502285*
- ²⁷*Indian Institute of Technology Madras, Chennai 600036*
- ²⁸*Indiana University, Bloomington, Indiana 47408*
- ²⁹*Institute of High Energy Physics, Chinese Academy of Sciences, Beijing 100049*
- ³⁰*Institute of High Energy Physics, Vienna 1050*
- ³¹*Institute for High Energy Physics, Protvino 142281*
- ³²*INFN—Sezione di Napoli, 80126 Napoli*
- ³³*INFN—Sezione di Torino, 10125 Torino*
- ³⁴*J. Stefan Institute, 1000 Ljubljana*
- ³⁵*Institut für Experimentelle Teilchenphysik, Karlsruher Institut für Technologie, 76131 Karlsruhe*
- ³⁶*Kavli Institute for the Physics and Mathematics of the Universe (WPI), University of Tokyo, Kashiwa 277-8583*
- ³⁷*Kennesaw State University, Kennesaw, Georgia 30144*
- ³⁸*Department of Physics, Faculty of Science, King Abdulaziz University, Jeddah 21589*
- ³⁹*Kitasato University, Sagami-hara 252-0373*
- ⁴⁰*Korea Institute of Science and Technology Information, Daejeon 34141*
- ⁴¹*Korea University, Seoul 02841*
- ⁴²*Kyungpook National University, Daegu 41566*
- ⁴³*P. N. Lebedev Physical Institute of the Russian Academy of Sciences, Moscow 119991*
- ⁴⁴*Faculty of Mathematics and Physics, University of Ljubljana, 1000 Ljubljana*
- ⁴⁵*Ludwig Maximilians University, 80539 Munich*
- ⁴⁶*Luther College, Decorah, Iowa 52101*
- ⁴⁷*Malaviya National Institute of Technology Jaipur, Jaipur 302017*
- ⁴⁸*University of Maribor, 2000 Maribor*
- ⁴⁹*Max-Planck-Institut für Physik, 80805 München*
- ⁵⁰*School of Physics, University of Melbourne, Victoria 3010*
- ⁵¹*University of Mississippi, University, Mississippi 38677*
- ⁵²*University of Miyazaki, Miyazaki 889-2192*
- ⁵³*Moscow Physical Engineering Institute, Moscow 115409*
- ⁵⁴*Graduate School of Science, Nagoya University, Nagoya 464-8602*
- ⁵⁵*Kobayashi-Maskawa Institute, Nagoya University, Nagoya 464-8602*
- ⁵⁶*Università di Napoli Federico II, 80126 Napoli*
- ⁵⁷*Nara Women's University, Nara 630-8506*
- ⁵⁸*National Central University, Chung-li 32054*
- ⁵⁹*National United University, Miao Li 36003*
- ⁶⁰*Department of Physics, National Taiwan University, Taipei 10617*
- ⁶¹*H. Niewodniczanski Institute of Nuclear Physics, Krakow 31-342*
- ⁶²*Nippon Dental University, Niigata 951-8580*
- ⁶³*Niigata University, Niigata 950-2181*
- ⁶⁴*Novosibirsk State University, Novosibirsk 630090*
- ⁶⁵*Osaka City University, Osaka 558-8585*
- ⁶⁶*Pacific Northwest National Laboratory, Richland, Washington 99352*
- ⁶⁷*Panjab University, Chandigarh 160014*
- ⁶⁸*Peking University, Beijing 100871*
- ⁶⁹*University of Pittsburgh, Pittsburgh, Pennsylvania 15260*
- ⁷⁰*Punjab Agricultural University, Ludhiana 141004*
- ⁷¹*Research Center for Nuclear Physics, Osaka University, Osaka 567-0047*
- ⁷²*Department of Modern Physics and State Key Laboratory of Particle Detection and Electronics, University of Science and Technology of China, Hefei 230026*
- ⁷³*Seoul National University, Seoul 08826*
- ⁷⁴*Showa Pharmaceutical University, Tokyo 194-8543*
- ⁷⁵*Soochow University, Suzhou 215006*
- ⁷⁶*Soongsil University, Seoul 06978*
- ⁷⁷*Sungkyunkwan University, Suwon 16419*
- ⁷⁸*School of Physics, University of Sydney, New South Wales 2006*
- ⁷⁹*Department of Physics, Faculty of Science, University of Tabuk, Tabuk 71451*
- ⁸⁰*Tata Institute of Fundamental Research, Mumbai 400005*
- ⁸¹*Department of Physics, Technische Universität München, 85748 Garching*

⁸²*School of Physics and Astronomy, Tel Aviv University, Tel Aviv 69978*⁸³*Toho University, Funabashi 274-8510*⁸⁴*Department of Physics, Tohoku University, Sendai 980-8578*⁸⁵*Earthquake Research Institute, University of Tokyo, Tokyo 113-0032*⁸⁶*Department of Physics, University of Tokyo, Tokyo 113-0033*⁸⁷*Tokyo Institute of Technology, Tokyo 152-8550*⁸⁸*Tokyo Metropolitan University, Tokyo 192-0397*⁸⁹*Utkal University, Bhubaneswar 751004*⁹⁰*Virginia Polytechnic Institute and State University, Blacksburg, Virginia 24061*⁹¹*Wayne State University, Detroit, Michigan 48202*⁹²*Yamagata University, Yamagata 990-8560*⁹³*Yonsei University, Seoul 03722*⁹⁴*Hiroshima University, Hiroshima 739-8511*

(Received 11 July 2020; revised 14 December 2020; accepted 22 February 2021; published 23 March 2021)

We report the first evidence for $X(3872)$ production in two-photon interactions by tagging either the electron or the positron in the final state, exploring the highly virtual photon region. The search is performed in $e^+e^- \rightarrow e^+e^-J/\psi\pi^+\pi^-$, using 825 fb^{-1} of data collected by the Belle detector operated at the KEKB e^+e^- collider. We observe three $X(3872)$ candidates, where the expected background is 0.11 ± 0.10 events, with a significance of 3.2σ . We obtain an estimated value for $\tilde{\Gamma}_{\gamma\gamma}\mathcal{B}(X(3872) \rightarrow J/\psi\pi^+\pi^-)$ assuming the Q^2 dependence predicted by a $c\bar{c}$ meson model, where $-Q^2$ is the invariant mass squared of the virtual photon. No $X(3915) \rightarrow J/\psi\pi^+\pi^-$ candidates are found.

DOI: [10.1103/PhysRevLett.126.122001](https://doi.org/10.1103/PhysRevLett.126.122001)

The charmoniumlike state $X(3872)$ has been observed in various interactions since its first observation in $B \rightarrow KJ/\psi\pi^+\pi^-$ decays [1]. Its spin, parity, and charge conjugation are determined to be 1^{++} [2], but its internal structure is still a puzzle [3,4]. Subsequent to the spin-parity determination, the $X(3872)$ has not been searched for in two-photon interactions because axial-vector particles are forbidden to decay to two real photons [5]. However, mesons with $J^{PC} = 1^{++}$ can be produced if one or both photons are highly virtual [6]—denoted as γ^* .

We perform the first search for a 1^{++} charmonium state in two-photon interactions using $e^+e^- \rightarrow e^+e^-X(3872)$, where one of the final-state electrons, referred to as a tagging electron, is observed, and the other scatters at an extremely forward (backward) angle and is not detected [7]. Such events are called single-tag events. The $X(3872)$ is reconstructed via its decay to $J/\psi\pi^+\pi^-$ ($J/\psi \rightarrow \ell^+\ell^-$). By measuring the momentum of the tagging electron, we measure the Q^2 dependence of $X(3872)$ production, where $-Q^2$ is the invariant mass squared of the virtual photon. If the $X(3872)$ has a molecular component in its structure, it must have a steeper Q^2 dependence than the regular $c\bar{c}$ state. Hence, the single-tag two-photon interactions provide information on the structure of this state. The value of the

two-photon decay width, obtained from this measurement, is sensitive to the internal structure of the $X(3872)$. Early attempts to calculate such decay widths for charmoniumlike exotic states have been reported in Ref. [8]. We also search for the $X(3915)$ in the same final state through the G -parity-violating $J/\psi\rho^0$ ($\rho^0 \rightarrow \pi^+\pi^-$) channel, as well as $J/\psi\omega$ ($\omega \rightarrow \pi^+\pi^-$) decay [9].

We use 825 fb^{-1} of data collected by the Belle detector operated at the KEKB e^+e^- asymmetric collider [10,11]. The data were taken at the $\Upsilon(nS)$ resonances ($n \leq 5$) and nearby energies, $9.43 < \sqrt{s} < 11.03 \text{ GeV}$.

The Belle detector is a general-purpose magnetic spectrometer [12,13]. Charged-particle momenta are measured by a silicon vertex detector and a cylindrical drift chamber. Electron and charged-pion identification relies on a combination of the drift chamber, time-of-flight scintillation counters, aerogel Cherenkov counters, and an electromagnetic calorimeter made of CsI(Tl) crystals. Muon identification relies on resistive plate chambers in the iron return yoke.

For Monte Carlo (MC) simulations, used to set selection criteria and derive the reconstruction efficiency, we use TREPSBSS [14,15] to generate single-tag $e^+e^- \rightarrow e^+e^-X(3872)$ events in which the $X(3872)$ decays to $J/\psi\pi^+\pi^-$ and J/ψ decays leptonically. For simulating radiative J/ψ decays, we use PHOTOS [16,17]. A GEANT3-based program simulates the detector response [18].

Since one final-state electron is undetected, we select events with exactly five charged tracks, each coming from the interaction point and having $p_T > 0.1 \text{ GeV}/c$, with two

Published by the American Physical Society under the terms of the Creative Commons Attribution 4.0 International license. Further distribution of this work must maintain attribution to the author(s) and the published article's title, journal citation, and DOI. Funded by SCOAP³.

or more having $p_T > 0.4$ GeV/ c , where p_T is the transverse momentum with respect to the e^+ direction.

J/ψ candidates are reconstructed by their decays to e^+e^- or $\mu^+\mu^-$. A charged track is identified as an electron if its electron likelihood ratio $\mathcal{L}_e/(\mathcal{L}_e + \mathcal{L}_\pi)$ is greater than 0.66 and as a muon if it is not selected as an electron and if its muon likelihood ratio $\mathcal{L}_\mu/(\mathcal{L}_\mu + \mathcal{L}_\pi + \mathcal{L}_K)$ is greater than 0.66; \mathcal{L}_x is the likelihood for a particle to be of species x [19,20]. We require the mass of the lepton pair to be in the range 3.047–3.147 GeV/ c^2 . In the calculation of the invariant mass of an e^+e^- pair, we include the four-momenta of radiated photons, having energy less than 0.2 GeV and angle relative to an electron direction of less than 0.04 rad.

The tagging electron must have an electron likelihood ratio greater than 0.95 or E/p greater than 0.87, where E is the energy measured by the electromagnetic calorimeter and p is the momentum of the particle. We require that the tagging electron have momentum above 1 GeV/ c and $p_T > 0.4$ GeV/ c . The electron momentum includes the momenta of radiated photons, using the same requirements as for the electrons from J/ψ decays.

We identify a charged track as a pion if it satisfies the likelihood ratio criteria of $\mathcal{L}_\pi/(\mathcal{L}_\pi + \mathcal{L}_K) > 0.2$, $\mathcal{L}_\mu/(\mathcal{L}_\mu + \mathcal{L}_\pi + \mathcal{L}_K) < 0.9$, $\mathcal{L}_e/(\mathcal{L}_e + \mathcal{L}_\pi) < 0.6$, and its E/p is less than 0.8 [21]. Events should have no photons with energy above 0.4 GeV or π^0 candidates with χ^2 from the mass-constrained fit less than 4.0.

As the $X(3872)$ should be back to back with the tagging electron projected in the plane perpendicular to the beam axis, we require the difference between their azimuthal angles be in the range $(\pi \pm 0.1)$ rad.

The total visible transverse momentum of the event p_T^* [22] should be less than 0.2 GeV/ c . We also require that the measured energy of the $J/\psi\pi^+\pi^-$ system E_{obs}^* be consistent with the expectation E_{exp}^* calculated from the momentum of the tagging electron and the direction and invariant mass of the $J/\psi\pi^+\pi^-$ system, imposing energy-momentum conservation. Since the energy and total transverse momentum are correlated, we impose a two-dimensional criterion

$$(p_T^* + 40 \text{ MeV}/c) \left(\frac{|E_{\text{obs}}^* - E_{\text{exp}}^*|}{E_{\text{exp}}^*} + 0.003 \right) < 3 \text{ MeV}/c. \quad (1)$$

Figure 1 shows the distribution of events and these selection criteria in the p_T^* vs $E_{\text{obs}}^*/E_{\text{exp}}^*$ plane.

Finally, we place a requirement on the missing momentum of the event, equal to the momentum of the unmeasured electron that goes down the beam pipe. We require the missing-momentum projection in the e^- beam direction in the center-of-mass frame be less than -0.4 GeV/ c for e^- -tagging events and greater than 0.4 GeV/ c for e^+ -tagging events.

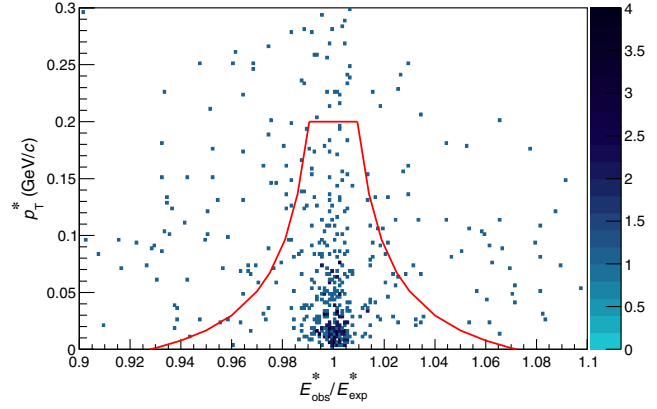


FIG. 1. p_T^* vs $E_{\text{obs}}^*/E_{\text{exp}}^*$ distribution from data. The (red) line shows the selection criteria applied to p_T^* and $E_{\text{obs}}^*/E_{\text{exp}}^*$; events below the line are accepted.

We search for $X(3872)$ and $X(3915)$ by looking for events in the $J/\psi\pi^+\pi^-$ mass distribution $M(J/\psi\pi^+\pi^-)$. The reconstructed mass resolution is expected to be 2.5 MeV/ c^2 from the MC simulation. We define two signal regions: 3.867–3.877 GeV/ c^2 for the $X(3872)$ and 3.895–3.935 GeV/ c^2 for the $X(3915)$. The former accommodates the $X(3872)$ with a known mass of 3871.69 ± 0.17 MeV/ c^2 and a decay width less than 1.2 MeV [23]; the latter accommodates the $X(3915)$ with a known mass of 3918.4 ± 1.9 MeV/ c^2 and a decay width of 20 ± 5 MeV. We constrain the J/ψ mass to 3.09690 GeV/ c^2 when we calculate $M(J/\psi\pi^+\pi^-)$ [24].

The dominant background, centered at 3.686 GeV/ c^2 , arises from radiatively produced $\psi(2S)$, $e^+e^- \rightarrow e^+e^-\psi(2S)$, with $\psi(2S) \rightarrow J/\psi\pi^+\pi^-$. Figure 2 shows the $M(J/\psi\pi^+\pi^-)$ distribution in data in the vicinity of $\psi(2S)$. Although the width of the $\psi(2S)$ peak is 2.7 MeV/ c^2 , it has a tail on the higher mass side. This feature was also seen in previous studies of $J/\psi\pi^+\pi^-$ produced by initial-state radiation (ISR) [25].

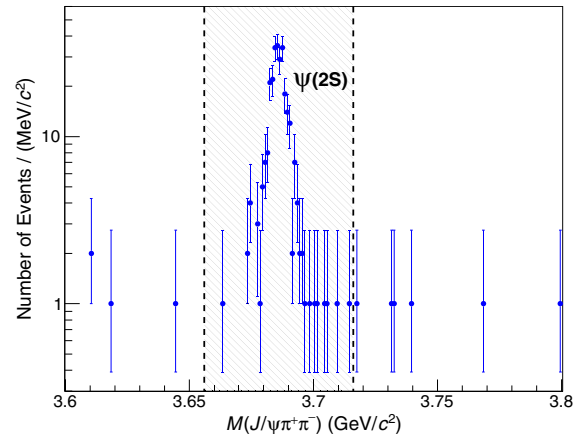


FIG. 2. $M(J/\psi\pi^+\pi^-)$ distribution shown with the $\psi(2S)$ veto (shaded gray region).

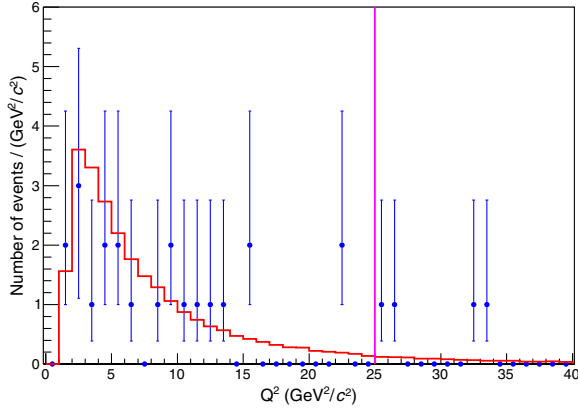


FIG. 3. Q^2 distribution for data (blue dots) and MC simulation (red histogram). The area of MC distribution is normalized to that of data. The vertical (magenta) line indicates the selection requirement.

To remove $\psi(2S)$ events, we veto events within $0.03 \text{ GeV}/c^2$ of the $\psi(2S)$ mass, $3.686 \text{ GeV}/c^2$. Figure 3 shows the Q^2 distribution after removing those events, where $Q^2 = 2(p_{\text{in}} \cdot p_{\text{out}} - m_e^2 c^2)$ and p_{in} and p_{out} are the four-momenta of the incoming (beam) and outgoing (tagging) electrons, and m_e is the electron mass. In Fig. 3, data are dominated by background events, while the MC simulation is pure $X(3872)$. Since two-photon processes are strongly suppressed at high Q^2 , we require $Q^2 < 25 \text{ GeV}^2/c^2$ to reduce non-two-photon background. Our measurement is insensitive for $Q^2 < 1.5 \text{ GeV}^2/c^2$ due to low reconstruction efficiency.

Figure 4 shows the observed events in the Q^2 vs $M(J/\psi\pi^+\pi^-)$ plane. Three events are in the $X(3872)$ signal region; no events are in the $X(3915)$ region. The masses of the events in the $X(3872)$ signal region are 3.8726 , 3.8701 , and $3.8742 \text{ GeV}/c^2$, averaging to $3.8723 \pm 0.0012 \text{ GeV}/c^2$, where the uncertainty is statistical. At masses below the $X(3872)$ region,

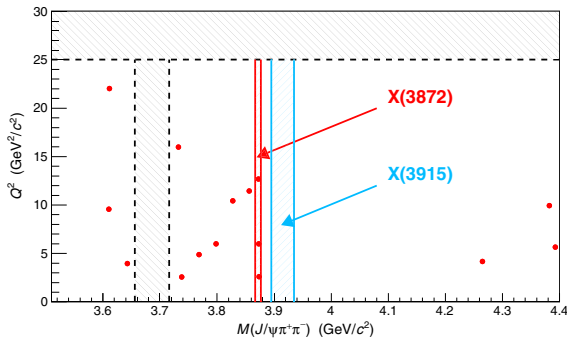


FIG. 4. Observed events (red dots) in the Q^2 vs $M(J/\psi\pi^+\pi^-)$ plane. Three events are seen in the $X(3872)$ signal region (red lines with shade). The blue lines with shade show the $X(3915)$ signal region. The vetoed regions are shaded gray with dashed lines.

$3.716\text{--}3.867 \text{ GeV}/c^2$, there are six events, presumably from $\psi(2S)$ events; at masses above the $X(3872)$, there are no events below $4.266 \text{ GeV}/c^2$, in the region of the $Y(4260)$ mass. A similar distribution was seen in the Belle ISR study [25]. The $J/\psi\pi^+\pi^-$ events can also originate from t -channel photon exchange with the emission of a virtual photon, which we call internal bremsstrahlung (IB) [26]. Both processes produce C -odd $J/\psi\pi^+\pi^-$, like $\psi(2S)$, while the C -even $X(3872)$ peak can only be produced from the two-photon process. The absence of a prominent $Y(4260)$ enhancement in our data argues against non-negligible contribution from the C -odd process through the decay $\gamma^* \rightarrow Y(4260) \rightarrow \gamma X(3872)$ [27]. To estimate the background from IB, which has the same final-state particle configuration as our process and is hence difficult to separate, we use the ISR data [25]. By fitting the ISR data to our data in the region $3.5 < M < 4.5 \text{ GeV}/c^2$, corrected for the differences in the diagrams of s and t channels, we estimate the number of background events to be $(3\text{--}5) \times 10^{-2}/(10 \text{ MeV}/c^2)$ in the region between 3.8 and $4.2 \text{ GeV}/c^2$. This explains the absence of events between the $X(3872)$ and $4.26 \text{ GeV}/c^2$.

To estimate the background level in the $X(3872)$ signal region, we fit a linear function

$$\max(0, a[M(J/\psi\pi^+\pi^-) - 3.872 \text{ GeV}/c^2] + b) \quad (2)$$

to the data in the region $\pm 0.156 \text{ GeV}/c^2$ centered at the $X(3872)$ mass, excluding the signal region; a and b are free in the fit. The width of $0.156 \text{ GeV}/c^2$ is determined by the distance between the $X(3872)$ and the upper boundary, $3.716 \text{ GeV}/c^2$, of the $\psi(2S)$ vetoed region. Using an unbinned extended maximum-likelihood fit, we obtain $a = -345 \pm 195/(\text{GeV}/c^2)^2$ and $b = 10.5 \pm 10.1/(\text{GeV}/c^2)$. This yields $n_b = 0.11 \pm 0.10$ background events in the $X(3872)$ signal window, where the uncertainty is statistical only.

To derive the systematic uncertainty due to background modeling, we test two modified fitting functions. One is a power function, $a'/[M(J/\psi\pi^+\pi^-) - b']^{c'}$ with b' set to $2.4 \text{ GeV}/c^2$; the fit is insensitive to the value of b' . This gives $n_b = 0.096 \pm 0.068$. The other is a linear function with a break at $3.800 \text{ GeV}/c^2$, $a''[M(J/\psi\pi^+\pi^-) - 3.800 \text{ GeV}/c^2] + b''$ for $M(J/\psi\pi^+\pi^-) < 3.800 \text{ GeV}/c^2$ and b'' for $M(J/\psi\pi^+\pi^-) \geq 3.800 \text{ GeV}/c^2$, based on the shapes of the $M(J/\psi\pi^+\pi^-)$ distributions in the ISR [25,28] and the e^+e^- annihilation studies [29,30]. This gives $n_b = 0.122 \pm 0.095$. From the variations of n_b in the three forms, we derive ± 0.013 for the systematic uncertainty. This is negligible compared to the statistical uncertainty. The estimated number of background events is 0.11 ± 0.10 , including statistical and systematic uncertainties.

With this background, the significance of three events is 3.2σ . For the $X(3872)$ signal, with three observed and 0.11

expected background events, we calculate the number of signal events, $N_{\text{sig}} = 2.9_{-2.0}^{+2.2}(\text{stat}) \pm 0.1(\text{syst})$, at 68% confidence level (C.L.). For the $X(3915)$ signal, with zero observed and 0.3 expected background events, we obtain $N_{\text{sig}} < 2.14$ at 90% C.L. The Feldman-Cousins method is used in both cases [31].

The differential cross section for the production of a resonance (X) in a single-tag two-photon interaction is expressed as [32]

$$\frac{d\sigma_{ee}(X)}{dQ^2} = 4\pi^2 \left(1 + \frac{Q^2}{M^2}\right) \frac{2J+1}{M^2} \Gamma_{\gamma^*\gamma}(Q^2) \times 2 \frac{d^2 L_{\gamma^*\gamma}}{dW dQ^2} \Big|_{W=M}, \quad (3)$$

where $L_{\gamma^*\gamma}$ is the single-tag luminosity function, M is the resonance mass, $-Q^2$ is the invariant mass squared of the virtual photon, $\Gamma_{\gamma^*\gamma}(Q^2)$ is the $\gamma^*\gamma$ decay width, W is the invariant mass of the $\gamma^*\gamma$ system, and J is the resonance spin. The factor of 2 comes from the existence of two production modes: $e^-\gamma^*$ and $e^+\gamma^*$ scattering.

For a $J = 1$ resonance, spin-parity conservation forbids production at $Q^2 = 0$. To remove the Q^2 dependence from $\Gamma_{\gamma^*\gamma}(Q^2)$, we use the reduced $\gamma\gamma$ decay width $\tilde{\Gamma}_{\gamma\gamma}$ defined as [6,33]

$$\tilde{\Gamma}_{\gamma\gamma} \equiv \lim_{Q^2 \rightarrow 0} \frac{M^2}{Q^2} \Gamma_{\gamma^*\gamma}^{LT}(Q^2), \quad (4)$$

using its Q^2 dependence near zero; $\Gamma_{\gamma^*\gamma}^{LT}$ is the $\gamma^*\gamma$ decay width corresponding to a formation of the resonance from a longitudinal (virtual) photon and a transverse (real) photon. Substituting this expression into Eq. (3), we obtain

$$\frac{d\sigma_{ee}(X)}{dQ^2} = 4\pi^2 \frac{3}{M^2} 2 \frac{Q^2}{M^2} \epsilon \tilde{\Gamma}_{\gamma\gamma} 2 \frac{d^2 L_{\gamma^*\gamma}}{dW dQ^2} \Big|_{W=M} \quad (5)$$

for $Q^2 \ll M^2$, where an extra factor of 2 comes from the difference in the number of spin degrees of freedom: the longitudinal component has one degree of freedom and the transverse component has two with unpolarized incident photons. In Eq. (5), ϵ is the ratio L^{LT}/L^{TT} , where L^{LT} is the luminosity function for the production of one longitudinally polarized photon and one transversely polarized photon, and L^{TT} is that for two transversely polarized photons. Using the Schuler-Berends-Gulik (SBG) model [6,34] for $q\bar{q}$ -type axial-vector mesons, this can be extended to higher Q^2 [33],

$$\frac{d\sigma_{ee}(X)}{dQ^2} = \tilde{\Gamma}_{\gamma\gamma} F(M, Q^2, \epsilon) \frac{d^2 L_{\gamma^*\gamma}}{dW dQ^2} \Big|_{W=M}, \quad (6)$$

where

$$F(M, Q^2, \epsilon) = \frac{48\pi^2}{M^2} \frac{\frac{Q^2}{2M^2} + \epsilon}{\left(1 + \frac{Q^2}{M^2}\right)^3} \frac{Q^2}{M^2}, \quad (7)$$

accounting for contributions from helicity 0 and 1. The SBG model, based on $c\bar{c}$, is the only model available at present that can reliably extend Eq. (5) to the higher Q^2 region: Eq. (7).

To relate the number of signal events and the decay width $\tilde{\Gamma}_{\gamma\gamma}$, we use Eqs. (6) and (7), assuming the $X(3872)$ is a pure $c\bar{c}$ state [6],

$$N_{\text{sig}} = L_{\text{int}} \mathcal{B}(X \rightarrow J/\psi \pi^+ \pi^-) \mathcal{B}(J/\psi \rightarrow \ell^+ \ell^-) \times \tilde{\Gamma}_{\gamma\gamma} \int_{Q_{\text{min}}^2}^{Q_{\text{max}}^2} dQ^2 F(M, Q^2, \epsilon) \epsilon_{\text{eff}}(Q^2) \frac{d^2 L_{\gamma^*\gamma}}{dW dQ^2} \Big|_{W=M}, \quad (8)$$

where $\epsilon_{\text{eff}}(Q^2)$ is the Q^2 -dependent reconstruction efficiency, L_{int} is the integrated luminosity, $\mathcal{B}(X \rightarrow J/\psi \pi^+ \pi^-)$ is the branching fraction of the $X(3872)$ to $J/\psi \pi^+ \pi^-$, and $\mathcal{B}(J/\psi \rightarrow \ell^+ \ell^-) = 0.1193$ is the branching fraction of J/ψ to lepton pairs [24]. We estimate the reconstruction efficiency from MC simulation, in which we model the $X(3872)$ decay as $X(3872) \rightarrow J/\psi \rho^0$ with $J/\psi \rightarrow \ell^+ \ell^-$ and $\rho^0 \rightarrow \pi^+ \pi^-$ and with all daughter particles isotropically distributed in the rest frames of their parents. The decay model via ρ is motivated by the measured mass distributions [1,35,36]. It has a reconstruction efficiency 12% higher than that for nonresonant $\pi^+ \pi^-$; we include a 6% systematic uncertainty to account for this. The angular distribution of the decay products of the $X(3872)$ negligibly affects the reconstruction, as confirmed by simulating with an alternative model with decay angles of daughters from a $J^P = 1^+$ resonance with helicities 0 and 1.

Detection efficiencies range from 4% to 8% for Q^2 between 3 and 25 GeV^2/c^2 and have smaller values for $Q^2 < 3 \text{ GeV}^2/c^2$. They are estimated for our three center-of-mass energies on the $\Upsilon(2S)$, $\Upsilon(4S)$, and $\Upsilon(5S)$ resonances and average the values weighted by their corresponding integrated luminosities. We also average over the four detection modes given the two tagging charges (e^+ and e^-) and the two J/ψ decay modes ($e^+ e^-$ and $\mu^+ \mu^-$).

The luminosity functions for our beam energies are calculated as functions of Q^2 using TREPSS. We set $\epsilon = 1$ as a convention for the present application of Eq. (7) [6]. After performing the Q^2 integration in Eq. (8), from $Q_{\text{min}}^2 = 1.5 \text{ GeV}^2/c^2$ to $Q_{\text{max}}^2 = 25 \text{ GeV}^2/c^2$, we obtain

$$\tilde{\Gamma}_{\gamma\gamma} \mathcal{B}(X(3872) \rightarrow J/\psi \pi^+ \pi^-) = (1.88 \pm 0.24) \text{ eV} \times N_{\text{sig}}, \quad (9)$$

including the total systematic uncertainty from the integration.

The dominant systematic uncertainty on $\tilde{\Gamma}_{\gamma\gamma}\mathcal{B}(X \rightarrow J/\psi\pi^+\pi^-)$ is from the reconstruction efficiency, primarily due to differences between MC simulation and data. The largest uncertainty, 7%, is in the J/ψ selection from the uncertainty of the e^+e^- background level. We estimate the total systematic uncertainty to be 13%.

From N_{sig} , we determine

$$\tilde{\Gamma}_{\gamma\gamma}\mathcal{B}(X(3872) \rightarrow J/\psi\pi^+\pi^-) = 5.5_{-3.8}^{+4.1}(\text{stat}) \pm 0.7(\text{syst}) \text{ eV.}$$

To set a limit on $\tilde{\Gamma}_{\gamma\gamma}$, we need $\mathcal{B}(X \rightarrow J/\psi\pi^+\pi^-)$. We derive an upper limit, using the measured products of B -meson decay branching fractions and the $X(3872)$ decay branching fractions $\mathcal{B}(B^+ \rightarrow K^+X)\mathcal{B}(X \rightarrow J/\psi\pi^+\pi^-)$ and other specific final states [37]. With the measured lower limit [24,35,38], this gives $0.032 < \mathcal{B}(X \rightarrow J/\psi\pi^+\pi^-) < 0.061$ at 90% C.L. Using the Feldman-Cousins method for three observed events and 0.11 background, we obtain $0.995 < N_{\text{sig}} < 7.315$ at 90% C.L. This, with Eq. (9), divided by $\mathcal{B}(X \rightarrow J/\psi\pi^+\pi^-)$, gives the $\tilde{\Gamma}_{\gamma\gamma}$ range: 20–500 eV. This is consistent with values predicted for the $c\bar{c}$ model [6,8]. For a comparison of experimental results with non- $c\bar{c}$ models, we must wait for improved calculations in the future.

No events consistent with $X(3915) \rightarrow J/\psi\pi^+\pi^-$ are observed. This, combined with past measurements [9,39], indicates no excess of G -parity-violating decays of $X(3915)$.

In summary, we find the first evidence for $X(3872)$ production in two-photon $\gamma^*\gamma$ interactions. We observe three $X(3872)$ candidates with a significance of 3.2σ and an estimated yield of $2.9_{-2.0}^{+2.2}(\text{stat}) \pm 0.1(\text{syst})$. From this, we obtain $\tilde{\Gamma}_{\gamma\gamma}\mathcal{B}(X(3872) \rightarrow J/\psi\pi^+\pi^-) = 5.5_{-3.8}^{+4.1}(\text{stat}) \pm 0.7(\text{syst}) \text{ eV}$, assuming the Q^2 dependence of a $c\bar{c}$ meson model. With future advances in calculations of $\tilde{\Gamma}_{\gamma\gamma}$ for non- $c\bar{c}$ states and higher luminosities accumulated by Belle II, we expect this method will clarify our understanding of the $X(3872)$.

We are grateful to M. Karliner for useful discussions. We thank the KEKB group for excellent operation of the accelerator, the KEK cryogenics group for efficient solenoid operations, and the KEK computer group, the NII, and PNNL/EMSL for valuable computing and SINET5 network support. We acknowledge support from MEXT, JSPS, and Nagoya's Tau-Lepton Physics Research Center (Japan); ARC (Australia); FWF (Austria); NSFC and Chinese Academy of Science Center for Excellence in Particle Physics (China); MSMT (Czechia); Carl Zeiss Foundation, DFG, EXC153, and VS (Germany); DST (India); INFN (Italy); MOE, MSIP, NRF, REST Society for Research International, FLRFAS project, GSDC of KISTI and Korea Research Environment Open Network/Global Ring Network for Advanced Application Development (Korea); MNiSW and NCN (Poland); Ministry of

Science and Higher Education of the Russian Federation, Agreement 14.W03.31.0026 (Russia); University of Tabuk (Saudi Arabia); ARRS (Slovenia); IKERBASQUE (Spain); SNSF (Switzerland); MOE and MOST (Taiwan); and DOE and NSF (U.S.).

- [1] S.-K. Choi *et al.* (Belle Collaboration), *Phys. Rev. Lett.* **91**, 262001 (2003).
- [2] R. Aaij *et al.* (LHCb Collaboration), *Phys. Rev. Lett.* **110**, 222001 (2013).
- [3] R. Aaij *et al.* (LHCb Collaboration), *Phys. Rev. D* **102**, 092005 (2020).
- [4] R. Aaij *et al.* (LHCb Collaboration), *J. High Energy Phys.* **08** (2020) 123.
- [5] The $X(3872)$ was searched for in two-photon interactions before its spin-parity determination: S. Dobbs *et al.* (CLEO Collaboration), *Phys. Rev. Lett.* **94**, 032004 (2005).
- [6] G. A. Schuler, F. A. Berends, and R. van Gulik, *Nucl. Phys.* **B523**, 423 (1998).
- [7] We use “electron” to denote both electron and positron.
- [8] T. Branz, R. Molina, and E. Oset, *Phys. Rev. D* **83**, 114015 (2011).
- [9] S. Uehara *et al.* (Belle Collaboration), *Phys. Rev. Lett.* **104**, 092001 (2010).
- [10] S. Kurokawa and E. Kikutani, *Nucl. Instrum. Methods Phys. Res., Sect. A* **499**, 1 (2003).
- [11] T. Abe *et al.* (KEKB Collaboration), *Prog. Theor. Exp. Phys.* **2013**, 03A001 (2013).
- [12] A. Abashian *et al.* (Belle Collaboration), *Nucl. Instrum. Methods Phys. Res., Sect. A* **479**, 117 (2002).
- [13] J. Brodzicka *et al.* (Belle Collaboration), *Prog. Theor. Exp. Phys.* **2012**, 04D001 (2012).
- [14] M. Masuda *et al.* (Belle Collaboration), *Phys. Rev. D* **93**, 032003 (2016).
- [15] S. Uehara, KEK Report No. 96-11, 1996, arXiv:1310.0157.
- [16] E. Barberio, B. van Eijk, and Z. Was, *Comput. Phys. Commun.* **66**, 115 (1991).
- [17] E. Barberio and Z. Was, *Comput. Phys. Commun.* **79**, 291 (1994).
- [18] R. Brun *et al.*, CERN Report No. DD/EE/84-1, 1987.
- [19] K. Hanagaki, H. Kakuno, H. Ikeda, T. Iijima, and T. Tsukamoto, *Nucl. Instrum. Methods Phys. Res., Sect. A* **485**, 490 (2002).
- [20] A. Abashian *et al.*, *Nucl. Instrum. Methods Phys. Res., Sect. A* **491**, 69 (2002).
- [21] E. Nakano, *Nucl. Instrum. Methods Phys. Res., Sect. A* **494**, 402 (2002).
- [22] The e^+e^- center-of-mass quantities are indicated by asterisks.
- [23] Recent measurements of the decay width show $\Gamma_{X(3872)}^{\text{BW}} = 0.96_{-0.18}^{+0.19} \pm 0.21 \text{ MeV}$ [3] and $\Gamma_{X(3872)}^{\text{BW}} = 1.39 \pm 0.24 \pm 0.10 \text{ MeV}$ [4].
- [24] N. Tanabashi *et al.* (Particle Data Group), *Phys. Rev. D* **98**, 030001 (2018), and 2019 update.
- [25] C. Z. Yuan *et al.* (Belle Collaboration), *Phys. Rev. Lett.* **99**, 182004 (2007), Fig. 1 shows $M(\ell^+\ell^-\pi^+\pi^-)$.
- [26] V. Bytev, E. Kuraev, E. Tomasi-Gustafsson, and Ping Wang, *Phys. Rev. D* **81**, 117501 (2010).
- [27] M. Ablikim *et al.* (BESIII Collaboration), *Phys. Rev. Lett.* **112**, 092001 (2014).

- [28] Z. Q. Liu *et al.* (Belle Collaboration), *Phys. Rev. Lett.* **110**, 252002 (2013), Fig. 1(a) inset shows $M(\ell^+\ell^-\pi^+\pi^-)$.
- [29] M. Ablikim *et al.* (BESIII Collaboration), *Phys. Rev. Lett.* **118**, 092001 (2017), Fig. 1 shows $M(\ell^+\ell^-\pi^+\pi^-)$.
- [30] N. E. Adam *et al.* (CLEO Collaboration), *Phys. Rev. Lett.* **96**, 082004 (2006), Fig. 1 shows $M(\ell^+\ell^-\pi^+\pi^-)$.
- [31] G. J. Feldman and R. D. Cousins, *Phys. Rev. D* **57**, 3873 (1998).
- [32] M. Masuda *et al.* (Belle Collaboration), *Phys. Rev. D* **97**, 052003 (2018).
- [33] H. Aihara *et al.* (TPC/2 γ Collaboration), *Phys. Rev. D* **38**, 1 (1988).
- [34] As a validation of the SBG model at higher Q^2 , Ref. [32] provides measurements of single-tag to no-tag ratios for the $\gamma\gamma$ decay widths for χ_{c0} and χ_{c2} , which agree with the predictions of this model.
- [35] S.-K. Choi *et al.* (Belle Collaboration), *Phys. Rev. D* **84**, 052004 (2011).
- [36] A. Abulencia *et al.* (CDF Collaboration), *Phys. Rev. Lett.* **96**, 102002 (2006).
- [37] From $\mathcal{B}(B^+ \rightarrow K^+X)\mathcal{B}(X \rightarrow J/\psi\pi^+\pi^-) = (8.6 \pm 0.6) \times 10^{-6}$ and the sum over the measured products of the branching fractions, $\mathcal{B}(B^+ \rightarrow K^+X)\mathcal{B}(X \rightarrow J/\psi\pi^+\pi^-, J/\psi\gamma, \psi(2S)\gamma, D^0\bar{D}^0\pi^0, \bar{D}^{*0}D^0) = (1.4 \pm 0.4) \times 10^{-4}$, where we exclude $\bar{D}^{*0} \rightarrow \bar{D}^0\pi^0$, we obtain that $\mathcal{B}(X \rightarrow J/\psi\pi^+\pi^-) < 0.061$ using the Bayesian method at 90% C.L. This limit is consistent with C. Li and C.-Z. Yuan, *Phys. Rev. D* **100**, 094003 (2019).
- [38] B. Aubert *et al.* (BABAR Collaboration), *Phys. Rev. D* **77**, 111101 (2008).
- [39] J. P. Lees *et al.* (BABAR Collaboration), *Phys. Rev. D* **86**, 072002 (2012).